On the clustering of bulk nanobubbles and their colloidal stability

Jadhav, Anand; Barigou, Mostafa

DOI:
10.1016/j.jcis.2021.05.154

Document Version
Peer reviewed version

Citation for published version (Harvard):
Jadhav, A & Barigou, M 2021, 'On the clustering of bulk nanobubbles and their colloidal stability', *Journal of Colloid and Interface Science*, vol. 601, pp. 816-824. https://doi.org/10.1016/j.jcis.2021.05.154

On the clustering of bulk nanobubbles and their colloidal stability

Ananda J. Jadhav, Mostafa Barigou✉

School of Chemical Engineering, University of Birmingham, Edgbaston,

Birmingham B15 2TT, United Kingdom

Abstract

Bulk nanobubbles which are usually observed in pure water have a mean diameter typically around 100 nm. We use a combination of physical and chemical techniques to prove the hypothesis that the nanoentities observed in pure water are stable clusters of much smaller stable nanobubbles. The stability of bulk nanobubble clusters is affected by factors such as ionic strength or internal energy of the system. We show that bulk nanobubbles on the order of 100 nm exist in a stable cluster form in neutral or basic media, and dissociate into tiny primary nanobubbles on the order of 1 nm in acidic media, or in the presence of small amounts of salt. These new findings suggest that bulk nanobubbles which have a high surface energy unsurprisingly tend to behave in a similar manner to solid nanoparticles in terms of their agglomeration tendency, which is confirmed by the DLVO theory. The results will have important implications for our understanding and interpretation of the behaviour of bulk nanobubbles, in particular their interfacial and colloidal stability.

Keywords: bulk nanobubbles; bulk nanobubble clusters; colloidal stability; DLVO theory; pH effects; salt effects.

✉Corresponding author; Email: m.barigou@bham.ac.uk

1. Introduction

Over that last decade, many authors including ourselves have reported the existence and persistence of a new class of nano-entities suspended in pure water, referred to as ultrafine bubbles or bulk nanobubbles (BNBs). BNBs can be generated by a number of different physical and chemical methods [1–14]. More recently, we have shown using various physical and chemical techniques that such nano-entities are indeed bubbles and cannot be attributed to any known form of impurity of contamination [1–3]. Similar to nanoparticles, they carry a significant negative surface charge which may be wholly or partly responsible for their extraordinary longevity [1,3,4,15]. We have also elucidated the effects of addition of surfactants, salts or pH adjustment on BNBs [2,4].

Thus, different surfactant molecules (non-ionic, anionic, cationic) affect BNBs in different ways. A non-ionic surfactant does not affect the nanobubble size distribution, number density or surface charge, but is expected to provide steric stabilisation to the suspension. An anionic surfactant does not affect the nanobubble number density or size distribution, but it is expected to enhance nanobubble stability by the so-called electro-steric stabilization mechanism as the surface charge increases with surfactant concentration. A cationic surfactant, on the other hand, gradually neutralises the surface potential leading to a charge reversal at the interface of the nanobubbles and, as a result, gives rise to complex effects on the nanobubble number density and size distribution. This is expected to destabilise the suspension at low surfactant concentrations, but stability is restored at higher concentrations as the surface charge increases again beyond the point of charge reversal [4].

The negatively charged nanobubble interface was postulated to create an external negative electrostatic pressure which balances the internal Laplace pressure so that, at equilibrium, no net gas diffusion occurs. The addition of a small amount of salt of any valence causes a sharp reduction in bubble number density and a sharp increase in mean bubble size. This effect which is more pronounced in the presence of a high salt valence, is attributed to a screening of the electric double layer formed by the co-ions which reduces the external negative electrostatic pressure causing a pressure imbalance across the interface of nanobubbles which then expand [1,3,4,16].

We also argued that in pure water, the adsorption of OH^- ions leads to the formation around the negatively charged BNBs of an electric double layer akin to that observed around solid

nanoparticles. The destabilisation of BNBs in an acidic medium was attributed to be the disruption of the equilibrium between the external electrostatic pressure and the inner Laplace pressure caused by a lower surface potential at low pH [1,3,4].

Thus, BNBs tend to be unstable and vanish in acidic media, whereas their stability is enhanced in basic media. Similarly, we showed that when a BNB suspension in water is subjected to a process of freezing followed by thawing, the BNBs disappear. The above findings have now culminated into the hypothesis that the observed nano-entities are not single nanobubbles but clusters of much smaller primary BNBs.

We here propose, therefore, to revisit some of our previous work to verify this hypothesis. Thus, we use a combination of experimental procedures to show that the nano-entities observed in pure water which are typically on the order 100 nm are clusters of tiny nanobubbles on the order of 1 nm, by demonstrating that: (i) when the pH of water is made acidic, the observed nano-entities disintegrate into tiny primary nanobubbles which recluster when the pH is neutralised or made basic; (ii) the addition of salt produces the same BNB cluster dissociation effects; (iii) freezing and thawing of the BNB suspension also causes all nano-entities in water to disintegrate into tiny nanobubbles which start to agglomerate quickly when subjected to vigorous shaking or slowly and gradually when stored undisturbed for a period of several days; and (iv) the encapsulation of BNBs with zinc phosphate produces hollow nanoparticles of a size range consistent with the observed primary nanobubbles and BNB clusters. Furthermore, we show that the DLVO theory gives a plausible description of the colloidal stability of BNBs.

2. Experimental

2.1 Materials

The water used in all experiments was ultrapure (type-1) water produced in a Millipore purification system (Avidity Science, UK), of electrical conductivity 0.055 $\mu S.cm^{-1}$ and pH 6.8 at a temperature of 20 ˚C. The pH of BNB suspensions produced in ultrapure water (hereafter called simply pure water) was adjusted using appropriate standard buffer solutions of pH4, pH7 and pH10. Buffer solutions of pH 7 (potassium dihydrogen phosphate/sodium hydroxide) and pH 10 (borax/sodium hydroxide) were procured from Fluka analytical (UK), whereas the buffer solution of pH 4 (phthalate) was procured from Acros organics (UK). Sodium chloride (NaCl, 99.5%) was purchased from Sigma Aldrich. Only reagents of the highest available purity grade were employed in experiments. Cleaning of glassware was

achieved by immersion for 30 min in a 10% aqueous solution of potassium hydroxide (KOH, Sigma Aldrich, UK) placed inside an ultrasonic bath, followed by rinsing with ultrapure water, drying in a microwave oven and flushing with a stream of high-purity dry nitrogen gas (BOC, UK). The purified water and all buffer stock solutions were initially examined prior to any experimentation for the presence of any nanoscale entities, using the Nanosight and Zetasizer instruments utilised for the characterisation of BNB suspensions, but no significant levels of impurity were detected. The Nanosight and Zetasizer are described further below.

2.2 Method of generation of BNB suspensions

BNB suspensions were produced in pure water using an expansion–compression method based on Henry's law principle of vacuum degasification, which is schematically illustrated in Figure 1 [2]. Initially, a syringe of appropriate size is filled with pure water and after expelling any air trapped within, the syringe tip is sealed using a Luer lock cap. The water is depressurised by quickly pulling out the syringe plunger and then repressurised by instant release of the plunger which travels at a relatively high velocity under the action of vacuum pressure; these two steps represent one full cycle of the BNB generation process. It should be noted that a sufficient amount of vacuum needs to be created inside the syringe in order to cause enough dissolved gas to be released as well as have enough pressure differential during the compression stage to enable the formation of BNBs. In other words, the pressure inside the syringe during the expansion stroke needs to be as low as possible. The concentration of BNBs generated depends on the number of expansion–compression cycles applied. Many successive cycles are required to produce a sufficiently large number of BNBs. Full details of the technique and its operation can be found in our recent paper [2].

2.3 Characterisation of BNB suspensions

To characterise the BNB suspensions, we used a combination of two popular techniques namely, nanoparticle tracking analysis and dynamic laser scattering, in a complimentary manner to enable us to cover the very wide range of BNB sizes encountered in this study.

2.3.1 Nanoparticle tracking analysis

A nanoparticle tracking analysis (NTA) technique (NanoSight NS300, Malvern-UK) was employed to measure the size distribution and the number density of BNBs. NTA utilizes the properties of both light scattering and Brownian motion to determine the size distribution of nanoparticles in liquid suspension. Tracking of the Brownian motion of nanoparticles makes

NTA ideally suited for real-time analysis of polydisperse suspensions ranging from 10 to 2000 nm in particle size and 10^7 to 10^9 particles.mL^{-1} in particle concentration. We have used this technique extensively and discussed its features and merits in more detail in our previous works [3,4].

2.3.2 Dynamic Light Scattering

Dynamic light scattering (DLS) is another suitable technique for the measurement of particles within a size range of 0.3 nm to 10 μm and a concentration range of 10^8 to 10^{12} particles.mL^{-1} [17,18]. The DLS instrument used here to determine the bubble size distribution of the BNB suspensions was ZEN5600 Zetasizer Nano ZSP (Malvern Instruments). DLS works on the principle that the Brownian motion of particles or molecules in suspension causes a laser light to be scattered at different intensities. Analysis of these intensity fluctuations yields the velocity of the Brownian motion and hence the particle size using the Einstein–Stokes relationship [19]. DLS, however, unlike NTA, does not measure the bubble number density. DLS can handle a wider range of BNB sizes and concentrations, but it tends to overestimate particle size and NTA is usually preferred, as discussed in our previous work [3]. Therefore, the DLS instrument was used here to mainly estimate bubble size at the lower end of the spectrum which NTA cannot detect, and to measure the zeta potential of BNBs, an important parameter in assessing their stability.

Standard suspensions of monosize solid latex nanospheres were used prior to analysis of nanobubble samples, to verify the accuracy and precision of the NTA and DLS systems and fine tune the settings of the instruments accordingly.

2.4 Evidence of BNB clustering

Our hypothesis is that BNBs produced in pure water exist in a cluster form, in other words, the nano-entities observed are nanoscale aggregates of much smaller primary nanobubbles. We herein employ a combination of physical and chemical experimental procedures to verify this hypothesis, as follows.

2.4.1 pH control of BNB suspension using buffer solutions

Experiments were conducted to study the effects of changing the pH of a BNB suspension produced in pure water, from neutral to acidic and then back to neutral by means of standard acidic and basic buffer solutions, on the bubble size distribution, mean bubble diameter, bubble number density and zeta potential. Thus, a 20 mL sample of BNB suspension generated in

pure water of initial pH 6.8 was placed in a clean glass bottle and its pH changed to acidic (pH 4) by dropwise addition of acidic buffer under gentle stirring. The sample was sealed and stirred further on a magnetic stirrer for 24 hrs and then analysed using NTA and DLS. Subsequently, the pH of the sample was changed back to neutral pH (~7.0) by dropwise addition of basic buffer, stirred further on a magnetic stirrer for 24 hr, and then analysed using NTA and DLS. Furthermore, using the same procedure, the pH was increased from neutral to basic (pH 10) by dropwise addition of basic buffer and the BNB sample analysed. It should be noted that prior to the above pH control experiments with the BNB suspension, the same experiments were run with just pure water to ascertain that the use of the acidic and basic buffers did not introduce any nanoscale impurities.

2.4.2 Addition of salt

A monovalent salt (NaCl) was added at different concentrations over the range 0.01 mM – 100 mM to check the effects on BNBs produced in pure water, to further verify the clustering hypothesis.

2.4.3 Freezing and thawing of BNB suspensions

Experiments conducted in this part of the study aimed to determine what happens to the initial mean bubble diameter and bubble number density when a BNB suspension produced in pure water was frozen at a temperature of −18 °C and then allowed to thaw at room temperature. Thus, samples of BNB suspension of 20 mL volume were kept in a freezer at −18 °C for a period of 24 h. The frozen samples were subsequently withdrawn and allowed to undergo thawing for about 6 h at room temperature before detailed analysis by NTA and DLS. Two types of BNB examination were conducted: (i) after thawing, a sample was stored and analysed daily over a period of 6 days; and (ii) similarly, after thawing, a sample was manually shaken vigorously and monitored over a period of 6 days.

2.4.4 Encapsulation of BNBs and TEM analysis

In this part of the study, BNBs formed in pure water were used as a soft template for the synthesis of hollow zinc phosphate nanoparticles. In a typical encapsulation procedure, two equal aliquots were taken from a BNB suspension to prepare two separate solutions containing, respectively, 33.4 mM of zinc nitrate (Zn $(NO_3)2{\cdot}6H_2O$) and 20 mM of diammonium phosphate ($(NH_4)_2HPO_4$). These two solutions were then slowly mixed and the pH of the mixture adjusted to 8.5 with aqueous ammonia, which resulted in the precipitation of white zinc-phosphate particles. The precipitate was recovered in a centrifuge, washed repeatedly

with water and ethanol, and then dried in an oven at 40 ˚C for 12 h. A transmission electron microscope (TEM) (JEOL 2100 TEM, Japan) with an acceleration voltage of 200 kV, was then employed to visualise the morphology of the synthesized particles, using standard TEM operating procedures [1].

3. Results and discussion

3.1 Effects of pH control using buffer solutions on BNB suspension

Figure 2 shows the size distribution, bubble number density, mean bubble diameter and zeta potential of the BNBs initially generated in pure water of pH 6.8, after adjusting the pH to 4 using the acidic buffer, and subsequently after adjusting the pH back to 6.8 using the basic buffer. At pH 4, the bubble size distribution curve collapses (Figure 2a) and the bubble number density falls drastically to near zero (Figure 2b), reaching the resolution limit of NTA at which it is not possible to reliably measure the bubble size distribution and estimate the mean bubble size (Figure 2c). The magnitude of the zeta potential of the BNBs decreases in absolute value from approximately −42 mV to −8 mV as the pH is reduced from 6.8 to 4 (Figure 2d), as expected given the increased acidity of the solution. These results are entirely consistent with our previous findings, in that BNBs seem to disappear at acidic pH but remain stable and visible at neutral and basic pH [2–4]. Here, we tested this phenomenon by readjusting the pH of the same suspension back to its original neutral value of ~7.0 using the basic buffer solution and analysed the BNBs using NTA and DLS. Results in Figure 2 show that the BNBs recover (within a small experimental error) their original size distribution, their number density, mean bubble size and zeta potential measured in pure water.

When the pH of the pure BNB suspension is increased from neutral to pH 10, however, no significant effects are observed on the BNB size distribution and bubble number density, as shown in Figure 2. The zeta potential slightly increases in absolute value because of the increased alkalinity of the solution.

These results seem to suggest that BNBs do actually survive in an acidic environment but their size is reduced below the resolution limit of the NTA which is not able to detect them. To confirm this supposition, we analysed the BNB suspensions using the DLS technique, because it can detect particle sizes down to 0.3 nm [17,18]. Figure 3 displays the bubble size distribution and mean bubble size measured by DLS of BNBs generated in pure water after adjusting their pH to 4 using the acidic buffer. These results show that at pH 4 BNBs do exist

but they are very small, with the mean diameter being on the order of ~1 nm. Such bubbles also enjoy long-term stability as depicted by their size distribution after 6 months. Therefore, it can be concluded that in an acidic medium BNBs exist as tiny stable primary nanobubbles, but in a neutral or basic medium such primary nanobubbles agglomerate to form much larger clusters on the order of 100 nm mean diameter. This behaviour is akin to that of nanoparticles. BNBs have a high surface area to volume ratio and, hence, a high surface energy. It is, therefore, not surprising that to minimize their surface energy, BNBs, like nanoparticles, tend to agglomerate [20]. Given the limited resolution of the available instruments, however, it is not possible to determine whether the primary nanobubbles are single bubbles or clusters of even smaller bubbles on the pico scale.

To demonstrate the gradual dissociation of the BNB clusters, the pH of the BNB suspension produced in pure water was adjusted to various levels within the range 4-10 and then analysed by NTA and DLS. Results depicted in Figure 4 show that the bubble number density falls off as pH is gradually reduced below neutral, and remains constant above neutral pH (Figure 4(a)). At the same time, the bubble size distribution shifts to the lower end of the spectrum as the BNB clusters disintegrate into smaller bubbles (Figure 4(b)), and the mean bubble diameter decreases from ~100 nm at neutral pH down to ~2 nm at pH 4 (Figure 4(c)).

In conclusion, NTA analysis shows that as the pH decreases, the stability of the BNB clusters decreases and the number density of BNB clusters reduces. However, by using DLS analysis, we have shown that bulk nanobubbles exist in a cluster form. The BNB clusters which seem to disappear because of their reduced stability, as observed by NTA, in fact, dissociate into smaller primary nanobubbles of a much smaller size, which cannot be detected by NTA as their size is below the resolution limit of the instrument. So, whilst the number of BNB clusters decreases in an acidic environment, primary nanobubbles arise as a result which are detected by DLS.

3.2 Effects of salt addition

The effects of adding a monovalent salt (NaCl) to a BNB suspensions produced in pure water are depicted in Figure 5. With increasing salt concentration, the bubble size distribution shifts radically to the left. At a concentration of 10 mM the BNB size has reached its minimum size (~1 nm) with no further reductions observed at higher concentrations. These results further

confirm the hypothesis that BNBs in pure water exist in a cluster form and start to dissociate into smaller bubbles in the presence of salt.

3.3 Effects of freezing and thawing on BNB suspensions

We previously reported that when BNBs produced in pure water were subjected to freezing followed by thawing, they seemed to disappear and we discussed the possible reasons for their disappearance [1,3,4]. We also stated that it was hard to tell whether the disappearance of the BNBs occurred during the freezing or thawing part of the process. Given that the freezing rate used was very low, we postulated that BNBs might conceivably be pressed together by growing crystals, in a way akin to the process of freeze concentration, so that they might coalesce or agglomerate causing eventually the BNBs to break up. However, it was much harder to speculate on a possible driver mechanism for nanobubble disappearance during the thawing stage of the experiment [3]. The above findings were based on NTA analysis of the BNB suspensions immediately or shortly after the process of thawing was complete.

To provide further evidence of BNB clustering, we here revisited the above work and investigated in more detail the effects of a freezing and thawing cycle on a BNB suspension produced in pure water. However, in this case we monitored the BNB suspensions after thawing over a long period of time. Results are summarised in Figure 6.

When a BNB suspension has been subjected to a freeze-thaw cycle, the bubble number density measured by NTA diminishes to vanishingly low levels. This seems to suggest that the observed nanobubbles either vanish completely or they dissociate into smaller bubbles of size below the detection limit of the NTA instrument. To verify these suppositions, we first analysed a freshly thawed sample after vigorous shaking. As shown in Figure 6, shaking seems to quickly trigger the reformation process causing a large proportion of the BNB clusters to reappear. The reformation process continues and is complete after six days when the bubble number density and the mean bubble diameter recover their initial values before freezing. In an undisturbed sample, however, the onset of cluster reformation is only visible after about four days and is complete after about six days. These results indicate that BNBs which are initially in the form of clusters, are broken up upon freezing and thawing into much smaller primary bubbles which survive the freeze-thaw process but are too small to be detected by NTA. Analysis of the thawed sample using DLS confirmed this interpretation, as shown in Figure 7, where after freezing and thawing the mean bubble size was reduced from its

initial size of ~100 nm down to ~2.9 nm. The results confirm the prior findings of the pH control and salt addition experiments described above, that in pure water BNBs do exist in cluster form.

3.4 Encapsulation of nanobubbles and TEM analysis

Sample TEM images of the precipitated white zinc-phosphate nanoparticles are presented in Figures 8. Each zinc-phosphate nanoparticle appears as a distinct light area (air domain) enclosed within a dark border region (solid shell). The TEM analysis, therefore, indicates that the zinc-phosphate nanoparticles are hollow and exist in a cluster form. The size of the primary zinc-phosphate nanoparticles ranges from about 3 to 150 nm, which is within the size range of the BNBs measured by NTA and DLS. The smaller particles are consistent with primary BNBs coated with zinc-phosphate, whereas the larger ones are consistent with BNB clusters coated with zinc-phosphate. This would be expected since the synthesis process combines an acidic (33.4 mM zinc nitrate) BNB solution with a basic (20 mM diammonium phosphate) BNB solution. The acidic BNB solution would be rich in tiny primary BNBs whereas the basic solution would contain large BNB clusters.

3.5 DLVO theory

We previously showed that the colloidal stability of air-water BNBs can be interpreted by the DLVO theory, as described in our recent work [4]. We use the DLVO theory here to explain the dissociation of BNB clusters into small primary nanobubbles. Using the results obtained in this study, the total interaction potential ($w_T(D)$) normalized by the microscopic kinetic energy of the molecules (k_BT) is plotted as a function of the dimensionless interspacing distance (κD) to demonstrate the effects of pH (Figure 9) and the effects of NaCl (Figure 10). The general trends of the interaction potentials, however, are depicted in Figure 11 for the purpose of discussion.

Like nanoparticles, BNBs have a high surface area to volume ratio and, hence, a high surface energy. To minimize their surface energy, therefore, they tend to agglomerate when they are in close proximity. This agglomeration or clustering process is facilitated by van der Waals attractive forces. The DLVO theory conjectures that when the spacing between BNBs is within the double-layer, the effect of van der Waals attractive forces is neutralised by electrostatic repulsive forces. Hence, the colloidal stability of BNBs will be governed by the summation of these forces as a function of BNB spacing (Figure 11). DLVO assumes the existence of two

energy minima (primary and secondary) where BNBs are stable, separated by an energy barrier determined by the combination of attractive and repulsive forces. As BNB spacing reduces, if BNBs are able to overcome the energy barrier, they would move to the primary minimum which is a preferred lower energy state for BNB clustering. Dissociation of the BNB clusters then becomes difficult as it requires significant energy input.

The attractive as well as repulsive forces are influenced by parameters such as ionic and dielectric strength of the solution which can be manipulated to control the energy barrier. Thus, BNBs in pure water are expected to be in stable cluster form in the primary minimum. Adjustment of pH or addition of salt, for example, causes the BNB clusters to dissociate and move to the secondary minimum as tiny stable bubbles. These phenomena are borne out by the experimental DLVO plots shown in Figures 9 and 10. For example, above pH 5, the energy barrier is positive and increases as pH increases (Figure 9), indicating movement towards a stable BNB cluster colloidal system at neutral pH. Increasing salt concentration, produces similar effects to reducing pH (Figure 10).

In conclusion, the DLVO theory seems to provide a reasonable interpretation of the colloidal stability of a BNB suspension, and support the hypothesis of the existence of BNBs in cluster form in pure water and their dissociation into much smaller nanobubbles with external input of energy.

4. Conclusions

We used a combination of physical and chemical techniques to show that BNBs in pure water exist in a stable cluster form, by demonstrating that: (i) in an acidic medium, the observed nano-entities dissociate into tiny nanobubbles on the order of ~1 nm and tend to regain their stable cluster form when the pH of the medium is made neutral or basic; (ii) the addition of salt produces the same BNB cluster dissociation effects; (iii) similarly, freezing followed by thawing causes all observed nano-entities suspended in water to disintegrate into tiny bubbles which again tend to recluster and recover their initial stable size quickly when vigorously shaken, or much more slowly and gradually if stored undisturbed for a period of time spanning several days; (iv) the encapsulation of the observed nano-entities with zinc phosphate produces hollow nanoparticles of a size range consistent with miniscule primary nanobubbles as well as large BNB clusters. It is not possible, however, to ascertain whether the primary nanobubbles are single bubbles or clusters of even smaller bubbles on the pico scale. The DLVO theory

seems to provide a plausible interpretation of the colloidal stability of a BNB suspension, and supports the hypothesis of the existence of BNBs in cluster form in pure water and their dissociation into much smaller nanobubbles with external input of energy.

CRediT authorship contribution statement

Mostafa Barigou: acquired the funding, conceived the research project and supervised the study. **Ananda Jadhav:** performed the experimental work and data analysis of nanobubble generation. Both authors contributed to the writing of the paper.

Declaration of competing interest

There are no conflicts of interest to declare.

Acknowledgements

This work was supported by EPSRC Grant EP/L025108/1.

References

[1] A.J. Jadhav, M. Barigou, Bulk Nanobubbles or Not Nanobubbles: That is the Question, Langmuir. 36 (2020) 1699–1708. https://doi.org/10.1021/acs.langmuir.9b03532.

[2] G. Ferraro, A. J. Jadhav, M. Barigou, A Henry's law method for generating bulk nanobubbles, Nanoscale. 12 (2020) 15869–15879. https://doi.org/10.1039/D0NR03332D.

[3] N. Nirmalkar, A.W. Pacek, M. Barigou, On the Existence and Stability of Bulk Nanobubbles, Langmuir. 34 (2018) 10964–10973. https://doi.org/10.1021/acs.langmuir.8b01163.

[4] N. Nirmalkar, A.W. Pacek, M. Barigou, Interpreting the interfacial and colloidal stability of bulk nanobubbles, Soft Matter. 14 (2018) 9643–9656. https://doi.org/10.1039/C8SM01949E.

[5] K. Yasuda, H. Matsushima, Y. Asakura, Generation and reduction of bulk nanobubbles by ultrasonic irradiation, Chemical Engineering Science. 195 (2019) 455–461. https://doi.org/10.1016/j.ces.2018.09.044.

[6] N.F. Bunkin, A.V. Shkirin, N.V. Suyazov, V.A. Babenko, A.A. Sychev, N.V. Penkov, K.N. Belosludtsev, S.V. Gudkov, Formation and Dynamics of Ion-Stabilized Gas Nanobubble Phase in the Bulk of Aqueous NaCl Solutions, J. Phys. Chem. B. 120 (2016) 1291–1303. https://doi.org/10.1021/acs.jpcb.5b11103.

[7] R. Etchepare, H. Oliveira, M. Nicknig, A. Azevedo, J. Rubio, Nanobubbles: Generation using a multiphase pump, properties and features in flotation, Minerals Engineering. 112 (2017) 19–26. https://doi.org/10.1016/j.mineng.2017.06.020.

[8] W.B. Zimmerman, V. Tesař, H.C.H. Bandulasena, Towards energy efficient nanobubble generation with fluidic oscillation, Current Opinion in Colloid & Interface Science. 16 (2011) 350–356. https://doi.org/10.1016/j.cocis.2011.01.010.

[9] A.K.A. Ahmed, C. Sun, L. Hua, Z. Zhang, Y. Zhang, W. Zhang, T. Marhaba, Generation of nanobubbles by ceramic membrane filters: The dependence of bubble size and zeta potential on surface coating, pore size and injected gas pressure, Chemosphere. 203 (2018) 327–335. https://doi.org/10.1016/j.chemosphere.2018.03.157.

[10] J. Qiu, Z. Zou, S. Wang, X. Wang, L. Wang, Y. Dong, H. Zhao, L. Zhang, J. Hu, Formation and Stability of Bulk Nanobubbles Generated by Ethanol-Water Exchange, Chemphyschem. 18 (2017) 1345–1350. https://doi.org/10.1002/cphc.201700010.

[11] J.C. Millare, B.A. Basilia, Dispersion and electrokinetics of scattered objects in ethanol-water mixtures, Fluid Phase Equilibria. 481 (2019) 44–54. https://doi.org/10.1016/j.fluid.2018.10.013.

[12] J.C. Millare, B.A. Basilia, Nanobubbles from Ethanol-Water Mixtures: Generation and Solute Effects via Solvent Replacement Method, ChemistrySelect. 3 (2018) 9268–9275. https://doi.org/10.1002/slct.201801504.

[13] J. Lombard, T. Biben, S. Merabia, Ballistic heat transport in laser generated nano-bubbles, Nanoscale. 8 (2016) 14870–14876. https://doi.org/10.1039/C6NR02144A.

[14] J. Jin, Z. Feng, F. Yang, N. Gu, Bulk Nanobubbles Fabricated by Repeated Compression of Microbubbles, Langmuir. 35 (2019) 4238–4245. https://doi.org/10.1021/acs.langmuir.8b04314.

[15] A.J. Jadhav, M. Barigou, Proving and interpreting the spontaneous formation of bulk nanobubbles in aqueous organic solvent solutions: effects of solvent type and content, Soft Matter. 16 (2020) 4502–4511. https://doi.org/10.1039/D0SM00111B.

[16] H. Zhang, Z. Guo, X. Zhang, Surface enrichment of ions leads to the stability of bulk nanobubbles, Soft Matter. 16 (2020) 5470–5477. https://doi.org/10.1039/D0SM00116C.

[17] V. Filipe, A. Hawe, W. Jiskoot, Critical Evaluation of Nanoparticle Tracking Analysis (NTA) by NanoSight for the Measurement of Nanoparticles and Protein Aggregates, Pharm Res. 27 (2010) 796–810. https://doi.org/10.1007/s11095-010-0073-2.

[18] Zetasizer Nano ZSP | Expert Colloid & Protein Characterization | Malvern Panalytical, (n.d.). https://www.malvernpanalytical.com/en/products/product-range/zetasizer-range/zetasizer-nano-range/zetasizer-nano-zsp (accessed May 6, 2020).

[19] B.J. Berne, R. Pecora, Dynamic Light Scattering: With Applications to Chemistry, Biology, and Physics, Dover Publications, 2000.

[20] A. Tsuda, N.K. Venkata, The role of natural processes and surface energy of inhaled engineered nanoparticles on aggregation and corona formation, NanoImpact. 2 (2016) 38–44. https://doi.org/10.1016/j.impact.2016.06.002.

Figure captions

Figure 1. Schematic representation of BNB generation process by means of successive expansion–compression cycles of pure water in a syringe: many cycles are required to achieve a high concentration of BNBs.

Figure 2. Effects of pH change on BNB suspension generated in pure water (NTA analysis): (a) bubble size distribution; (b)bubble number density; (c) mean bubble diameter; (d) zeta potential.

Figure 3. Bubble size distribution in acidic (pH 4) BNB suspension (DLS analysis).

Figure 4. Effects of pH adjustment on BNB suspension generated in pure water: (a) bubble number density (NTA analysis); (b) bubble size distribution; and (c) mean bubble diameter (DLS analysis).

Figure 5. Effects of addition of monovalent salt (NaCl) on BNB suspension generated in pure water (DLS analysis): (a) bubble size distribution; (b) mean bubble diameter.

Figure 6. Freeze. Effects of freezing and thawing on BNB suspension generated in pure water (NTA analysis): (a) bubble number density; (b) mean bubble diameter.

Figure 7. Bubble size distribution after freeze-thawing cycle of BNB suspension generated in pure water (DLS analysis).

Figure 8. TEM images of hollow zinc phosphate nanoparticles obtained by encapsulation of BNBs shown on different scales.

Figure 9. Effects of pH on DLVO interaction potentials of bulk nanobubbles initially generated in pure water: (b) is enlarged view of (a).

Figure 10. Effects of addition of NaCl on DLVO interaction potentials of bulk nanobubbles initially generated in pure water: (b) is enlarged view of (a).

Figure 11. DLVO theory: combination of van der Wall’s attractive forces and electrostatic repulsive forces governs interaction of BNBs.

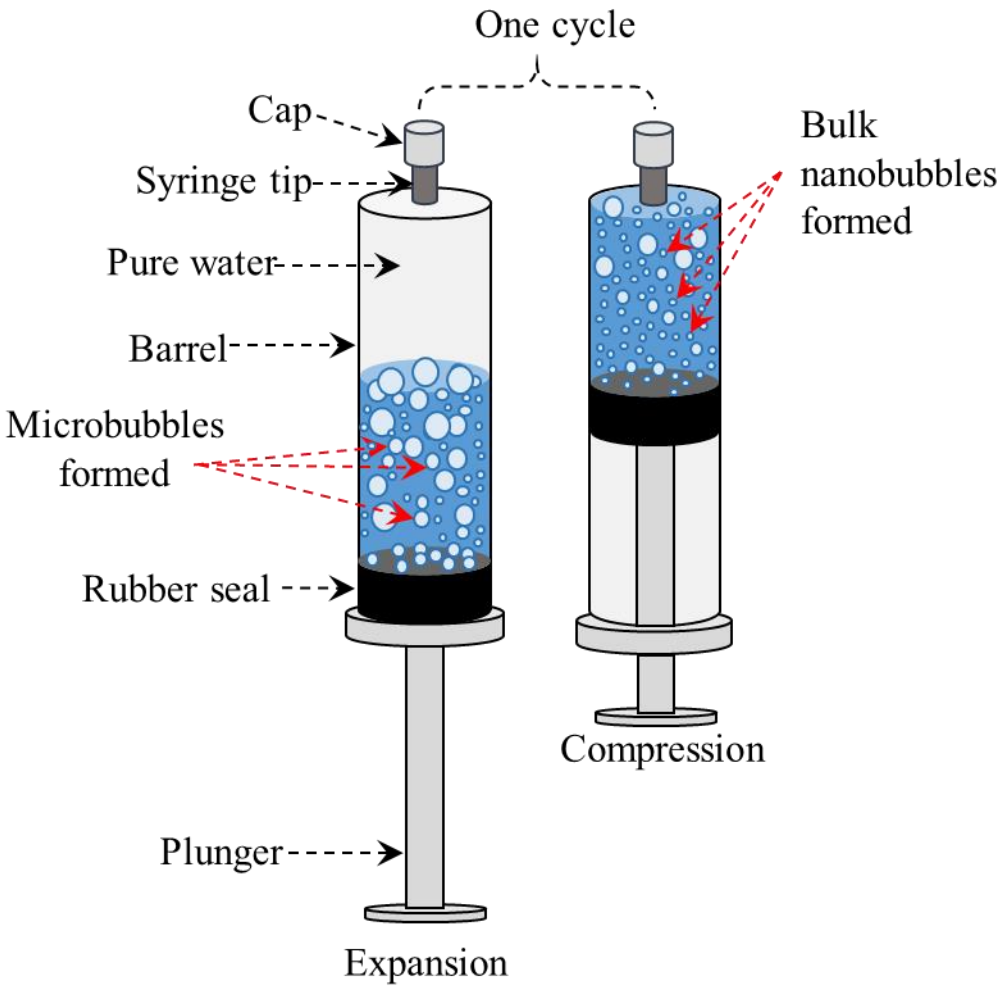

Figure 1. Schematic representation of BNB generation process by means of successive expansion–compression cycles of pure water in a syringe: many cycles are required to achieve a high concentration of BNBs.

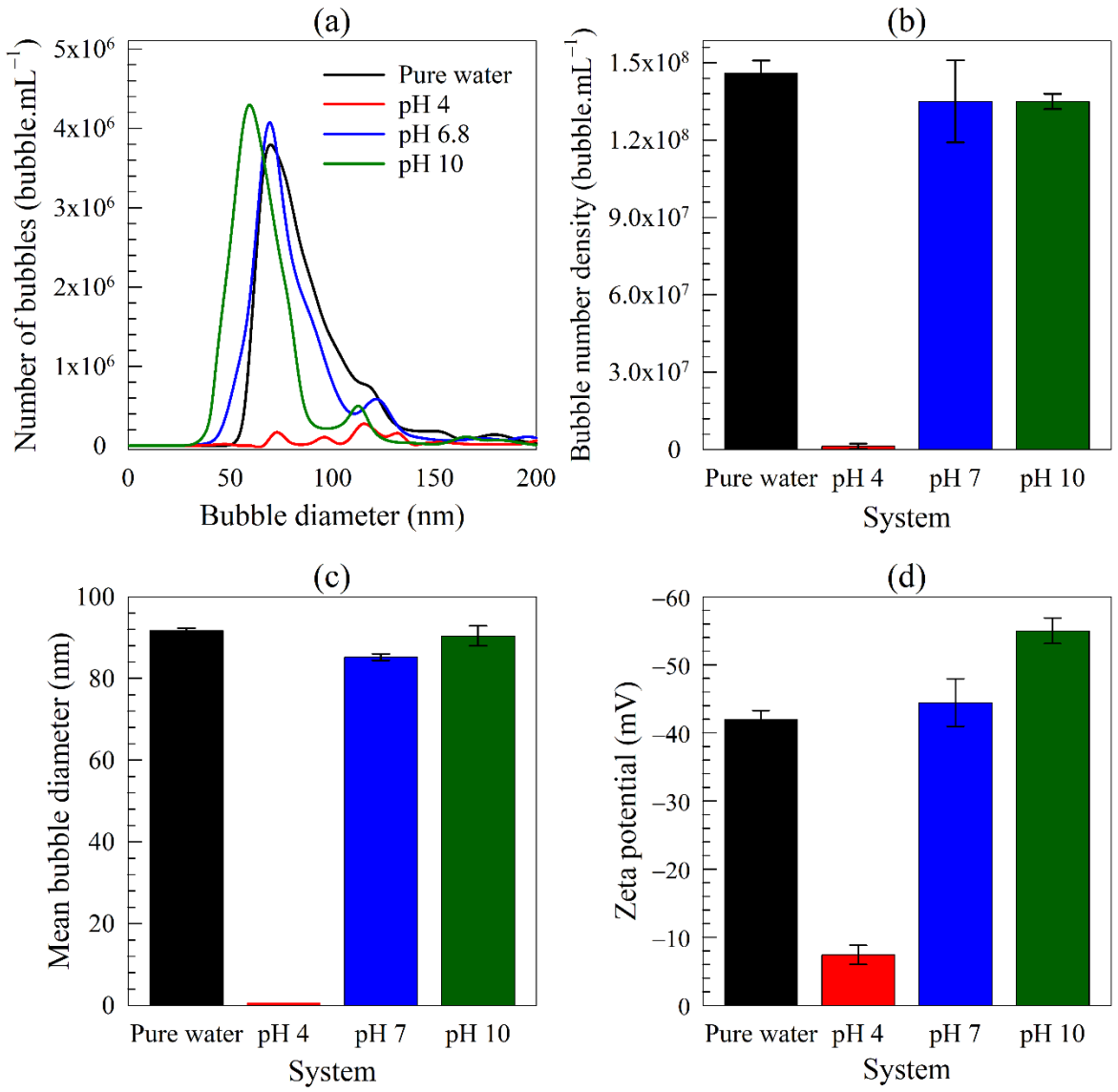

Figure 2. Effects of pH change on BNB suspension generated in pure water (NTA analysis): (a) bubble size distribution; (b)bubble number density; (c) mean bubble diameter; (d) zeta potential.

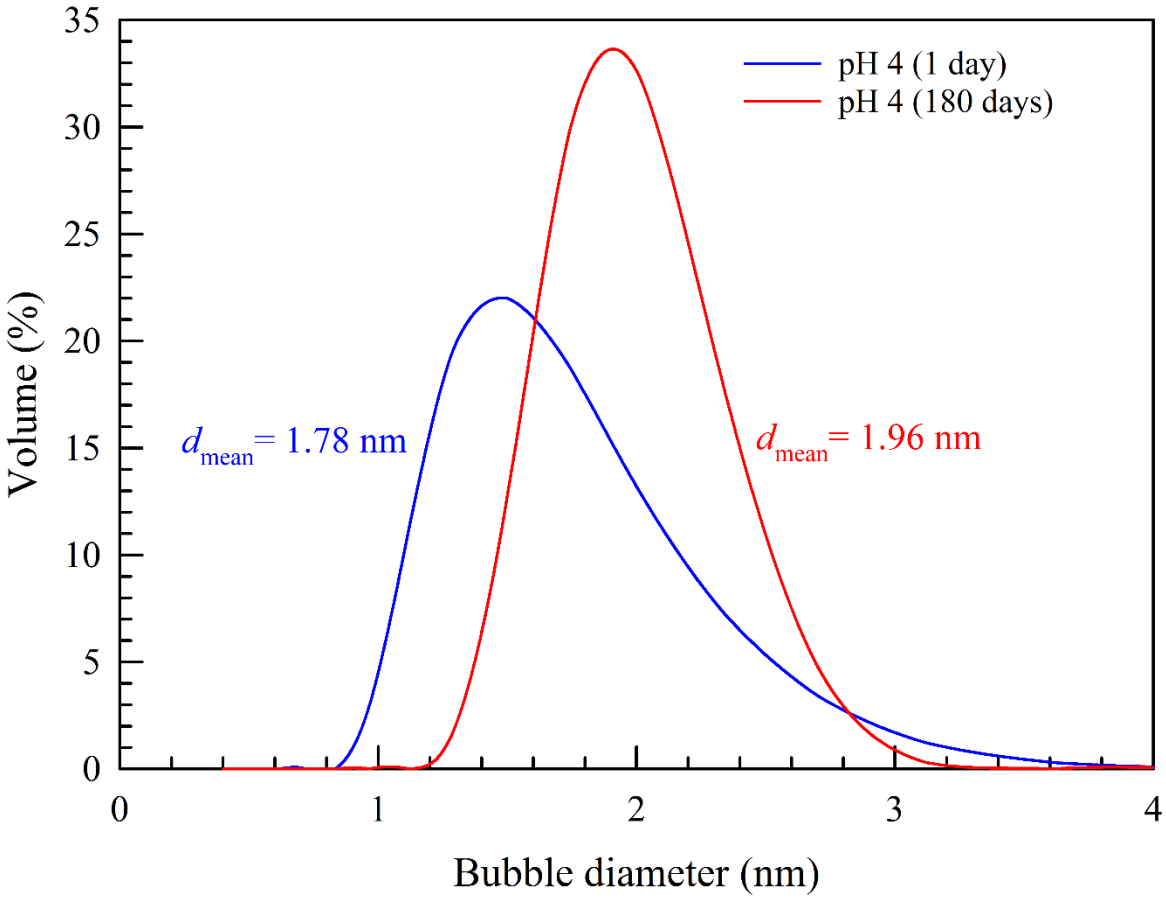

Figure 3. Bubble size distribution in acidic (pH 4) BNB suspension (DLS analysis).

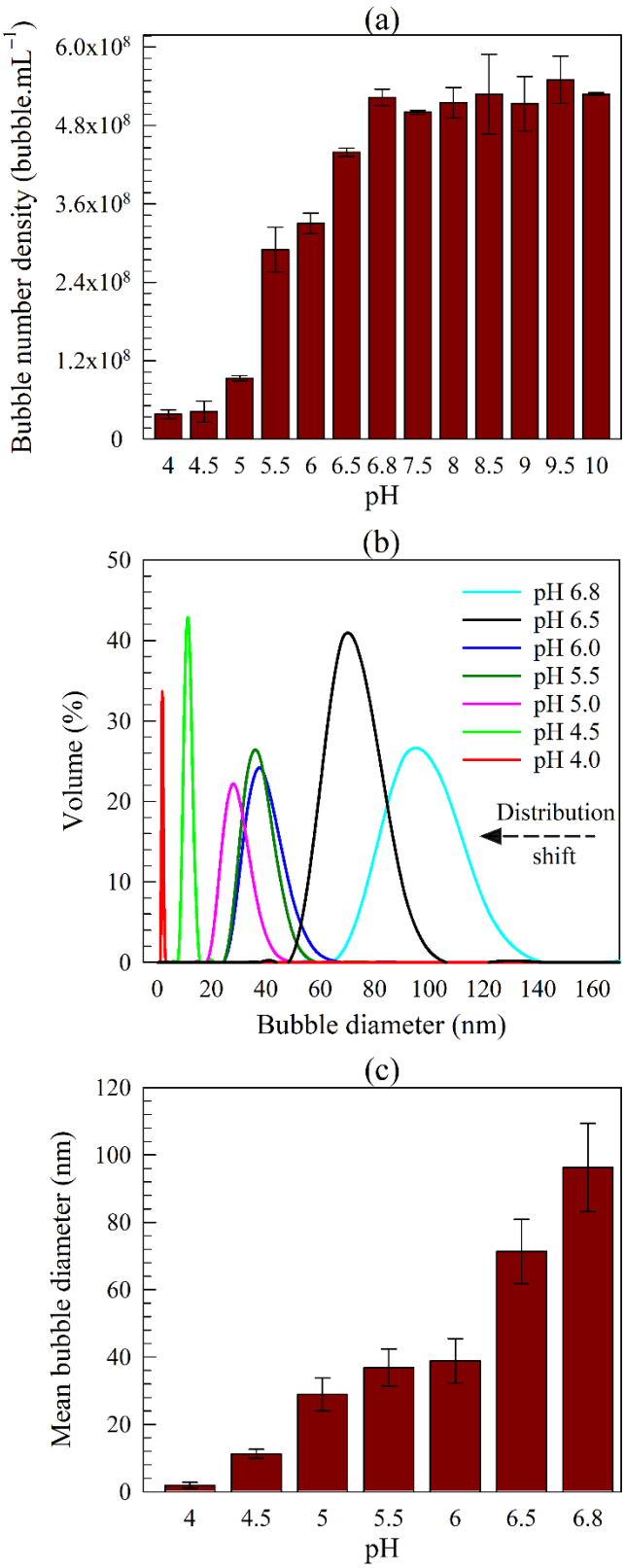

Figure 4. Effects of pH adjustment on BNB suspension generated in pure water: (a) bubble number density (NTA analysis); (b) bubble size distribution; and (c) mean bubble diameter (DLS analysis).

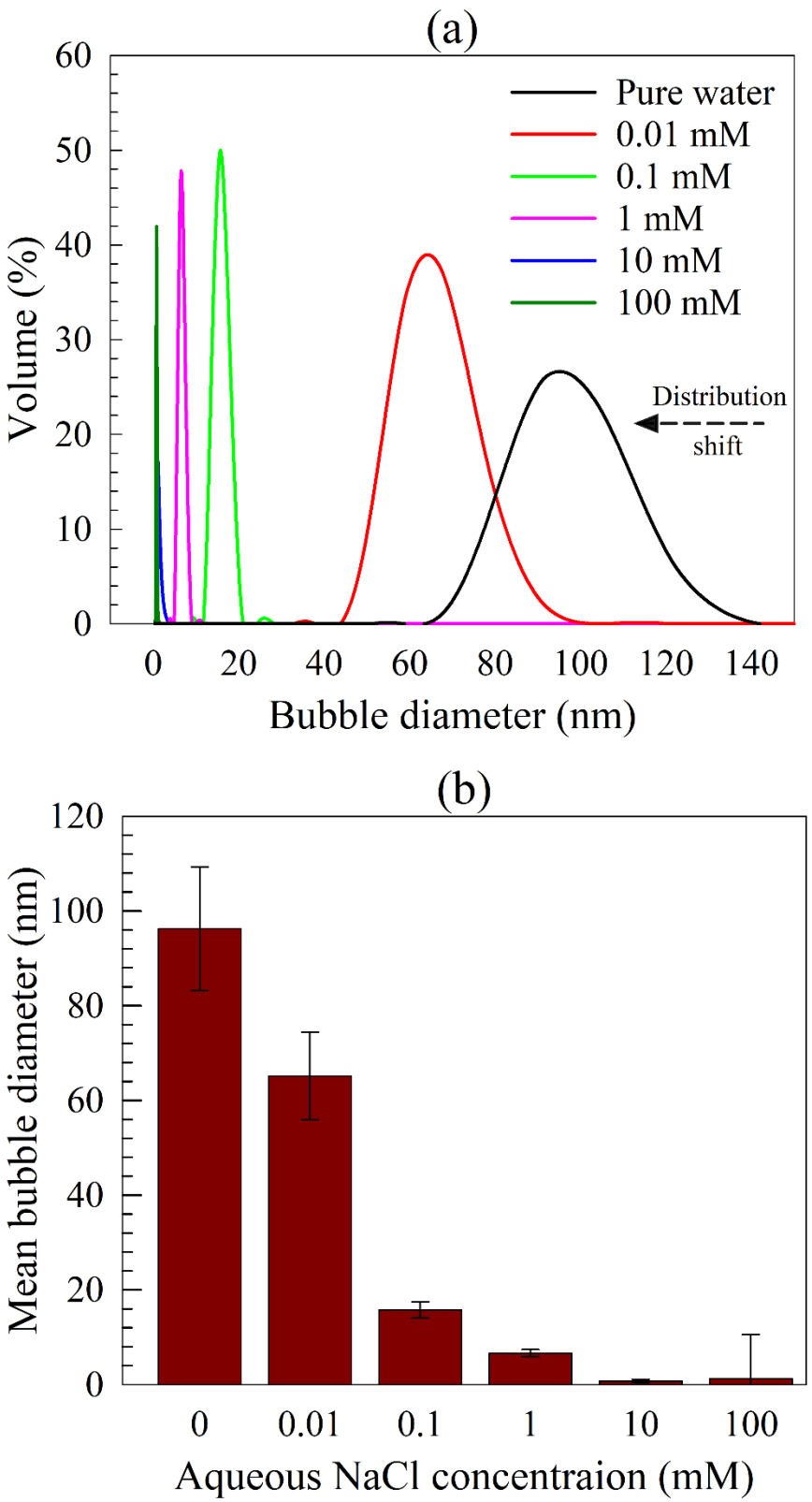

Figure 5. Effects of addition of monovalent salt (NaCl) on BNB suspension generated in pure water (DLS analysis): (a) bubble size distribution; (b) mean bubble diameter.

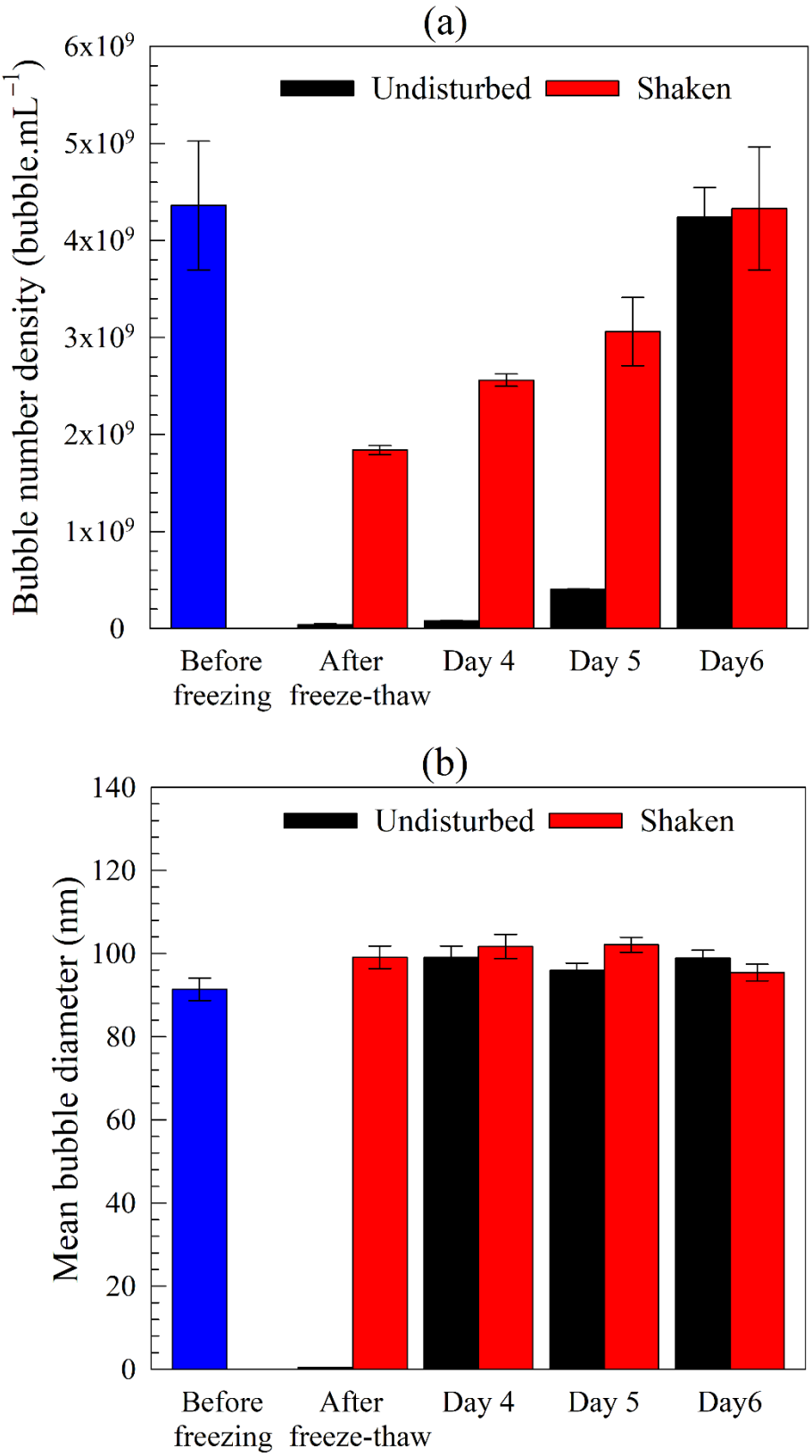

Figure 6. Freeze. Effects of freezing and thawing on BNB suspension generated in pure water (NTA analysis): (a) bubble number density; (b) mean bubble diameter.

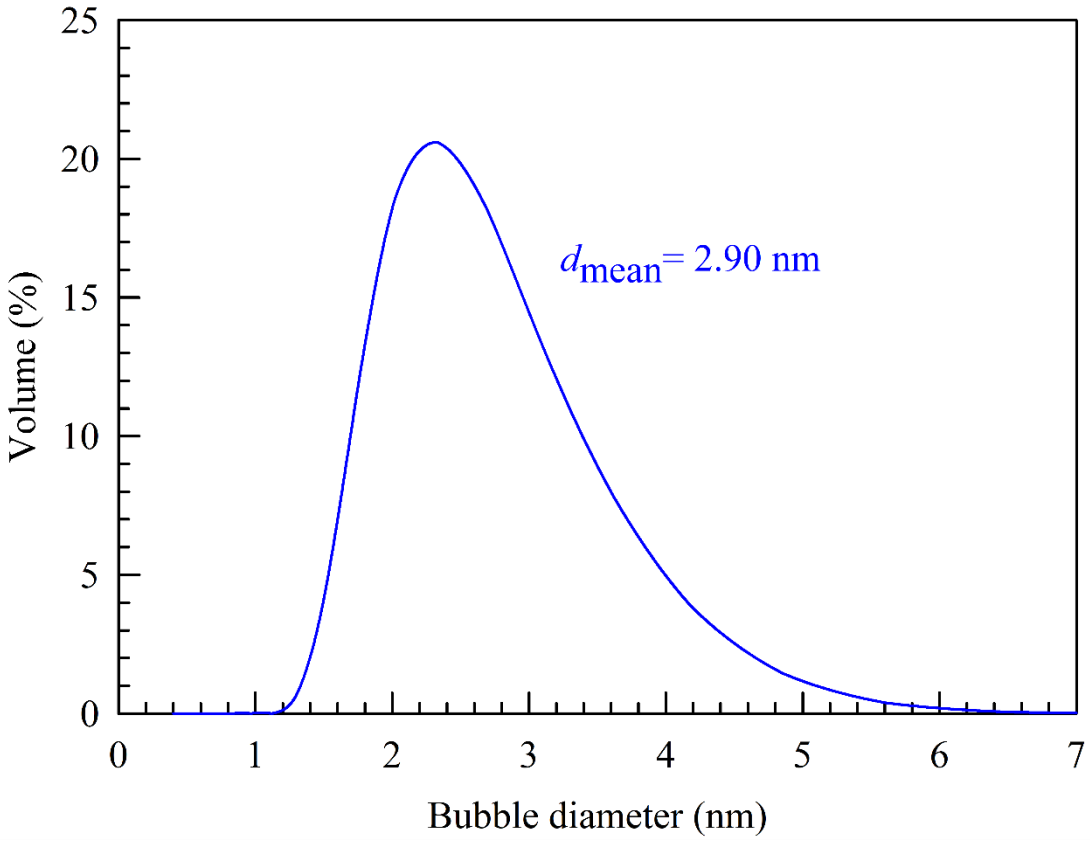

Figure 7. Bubble size distribution after freeze-thawing cycle of BNB suspension generated in pure water (DLS analysis).

(a)

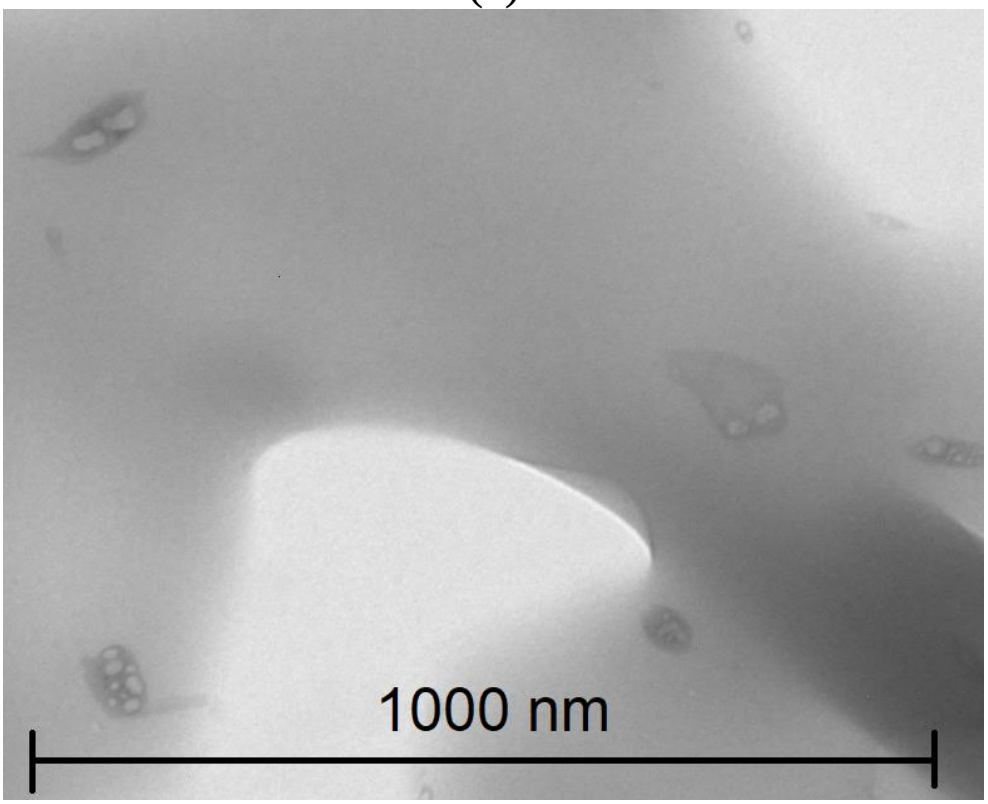

(b)

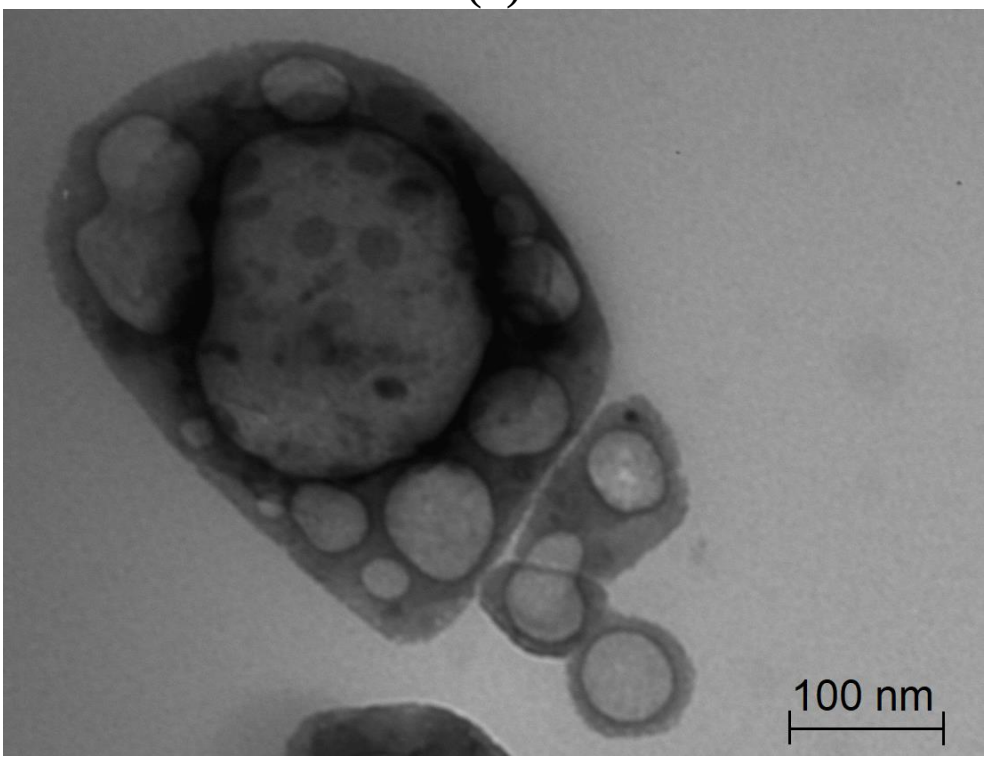

Figure 8. TEM images of hollow zinc phosphate nanoparticles obtained by encapsulation of BNBs shown on different scales.

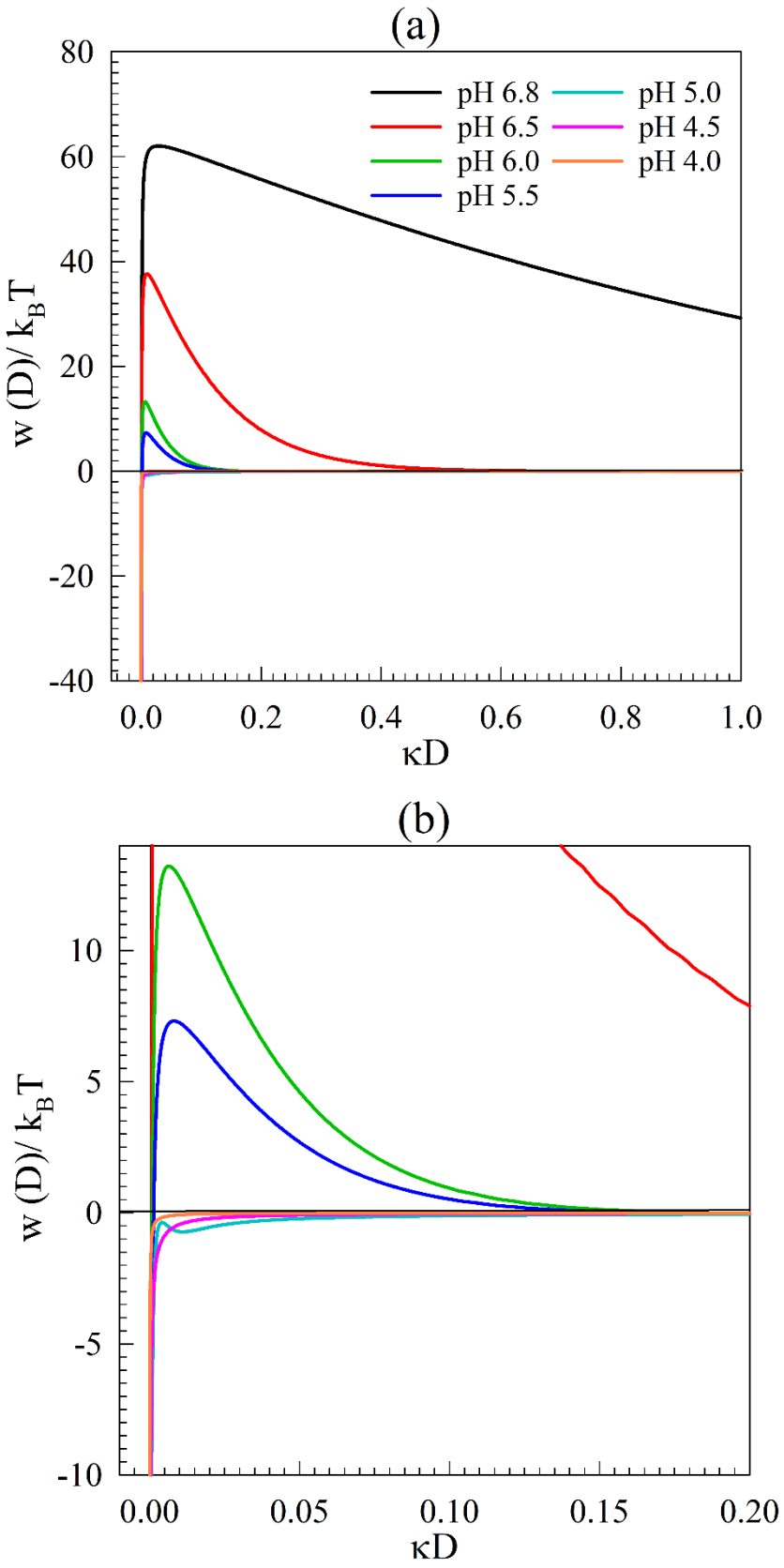

Figure 9. Effects of pH on DLVO interaction potentials of bulk nanobubbles initially generated in pure water: (b) is enlarged view of (a).

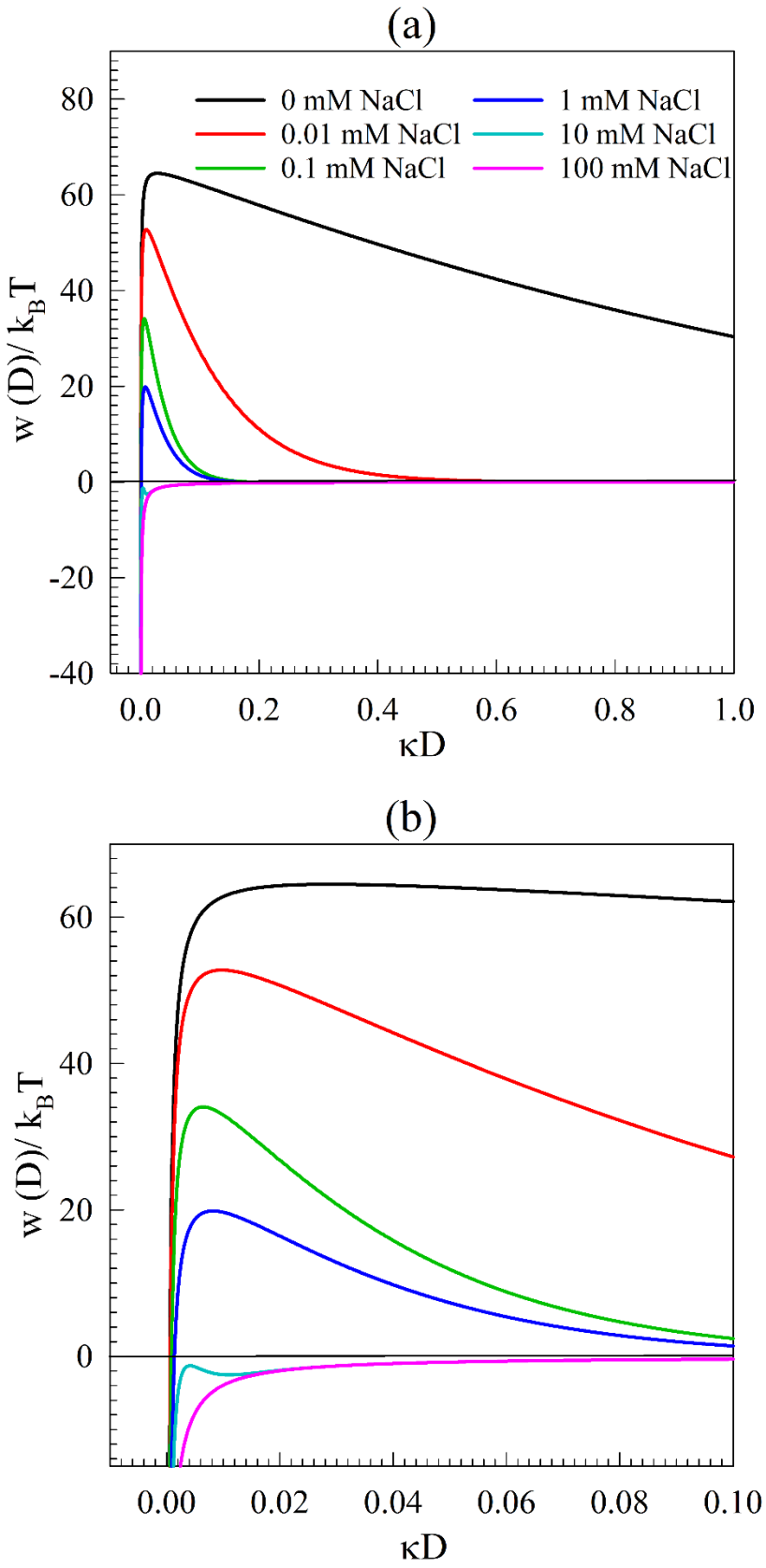

Figure 10. Effects of addition of NaCl on DLVO interaction potentials of bulk nanobubbles initially generated in pure water: (b) is enlarged view of (a).

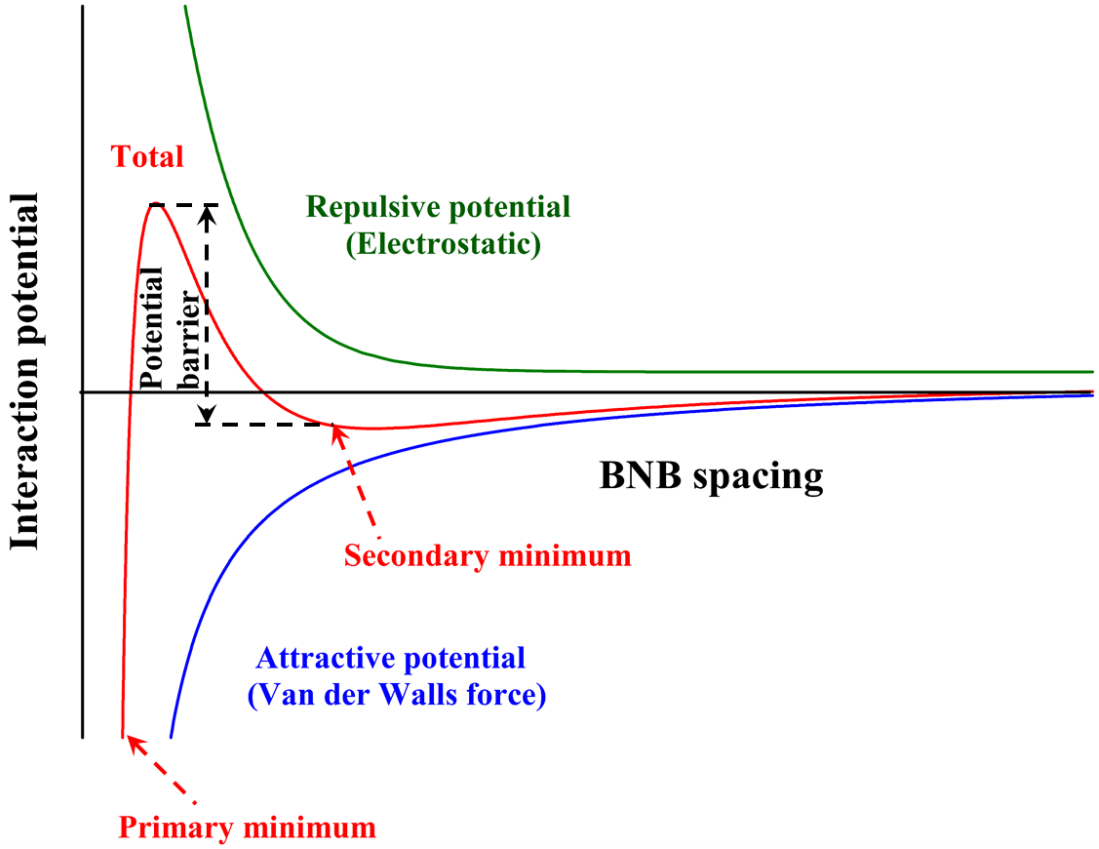

Figure 11. DLVO theory: combination of van der Wall's attractive forces and electrostatic repulsive forces governs interaction of BNBs.